Scaling properties of the area distribution functions and kinetic curves of dense plane discrete Poisson-Voronoi tessellations

A. Korobov*

Materials Chemistry Department, V. N. Karazin Kharkov National University, Kharkov 61022, Ukraine

(Received 17 October 2012; published 4 January 2013; corrected 1 February 2013)

This brief report supplements and refines previous publications [Korobov, Phys. Rev. B **76**, 085430 (2007); Korobov, Phys. Rev. E **79**, 031607 (2009); **84**, 021602 (2011)] to show that the scaling properties of the area distribution functions and kinetic curves actually hold for dense plane discrete Poisson-Voronoi tessellations. The previously noted apparent violations are due to the involved structures of boundaries of random domains.

DOI: 10.1103/PhysRevE.87.014401 PACS number(s): 81.15.Aa, 05.20.Dd, 02.50.Ey

Poisson-Voronoi tessellations serve as a basis for developing more involved and realistic descriptions of birth-growth processes, both analytical and numerical [1–8]. This, in turn, stimulates further studies of these tessellations in various respects [9–18]. All mentioned works deal with the Euclidean metric. Some problems require different metrics. One example is the evolution of a first-order phase transition on the sphere [19]. Another one is the account of the crystal structure of a substrate when its influence is tangible [20–22]. In the latter two-dimensional case, tessellations are discrete and are characterized by the density Λ, which is the ratio of the number of nucleation tiles to the total number of tiles in the tiling; $\Lambda < 1$. For sparse tessellations ($\Lambda < 0.01$) of hexagonal, square, and triangular tilings, the area distributions were shown to be practically metric insensitive, in contrast to metric sensitive kinetic characteristics. The parameter c of the Kiang conjecture [23]

$$F(y) = \frac{c^c}{\Gamma(c)} y^{c-1} \exp(-cy) \tag{1}$$

is close to that analytically derived for conventional continual tessellations with the Euclidian metric, $c = 3.575$ [24]. However, in the case of dense tessellations ($\Lambda \geqslant 0.01$, with a relatively large number of nuclei), the value of c is significantly different and kinetic curves of sparse and dense tessellations are not scaled one into another. This casts doubt on the universal behavior of discrete tessellations that is well established in the conventional case (see, e.g., [25,26]) and plays an important role when scaling properties of distribution functions are concerned [27–29]. The aim of this brief report is to settle this doubt and to show that the apparent violation of the universality is determined solely by some computational problems with boundaries of random domains.

The main features of the model are as follows (see [20–22] for more details): square tiling, simultaneous nucleation, one-tile stable nuclei, random distribution of nuclei, von Neumann neighborhood, irreversible linear growth to impingement, immobile islands. Several aspects of nucleation on square and triangular lattices are discussed in [30]. The von Neumann neighborhood is determined by the displacement vector:

$$N_5 = \left\{ \begin{pmatrix} 0 \\ 0 \end{pmatrix}; \begin{pmatrix} 1 \\ 0 \end{pmatrix}; \begin{pmatrix} 0 \\ 1 \end{pmatrix}; \begin{pmatrix} -1 \\ 0 \end{pmatrix}; \begin{pmatrix} 0 \\ -1 \end{pmatrix} \right\}. \tag{2}$$

At each step s, standing for discrete time, all adjacent tiles join the growing nucleus, forming the subsequent concentric belt around it. The growth is linear. In a topological respect, a peculiarity is the finite number of growth directions, whereas in continual two-dimensional nucleation growth models this number is infinite. In a metrical respect, a peculiarity is the fact that the discrete growth mode determines the metric which is different from the Euclidean metric: $\text{dist} = |\Delta x| + |\Delta y|$. It is impossible to construct a tessellation with habitual linear boundaries of random domains. There are two possibilities: boundaries are formed solely by tiles or boundaries are formed partly by lines and partly by tiles. The former case is computationally simpler and is considered here. It requires that the coordinates of all nuclei have the same evenness. Boundary tiles may possess fairly high multiplicity (the number of equidistant nuclei) and form two-dimensional arrays. The ratio of their number to the total number of tiles in the tiling considerably increases with the increase of Λ: 2.4, 8, 21.4, and 49.3% for Λ equals 0.0001, 0.001, 0.01, and 0.1 respectively [21].

To clarify the above problem, the area distribution functions and kinetic curves have been computed for tiles with the multiplicity 1 alone. To ensure consistency with previous publications, the statistical level of computations is the same as described in [20] (p. 5). The area of each random domain is simply the number of tiles belonging exclusively to this domain; the nucleation tile is included. Thus, computed areas S have been scaled as $S/\bar{S}$ (where $\bar{S}$ is the mean area of random domains), and the histogram constructed from these data has been normalized to the unit area. Note that $\bar{S}$ has been computed accounting for all tiles, both interior and boundary, which assumes the same partitioning of tilings as before [20,21]. The fraction of the interior tiles depends on Λ, as indicated above. Results for four different values of Λ are collected in Fig. 1. The solid line corresponds to the Kiang conjecture in Eq. (1), with $c = 3.575$. The fit is equally good for all values of Λ. Recall that when boundary tiles were taken into account $c = 6.1$ for $\Lambda = 0.1$ [21].

*Alexander.I.Korobov@univer.kharkov.ua

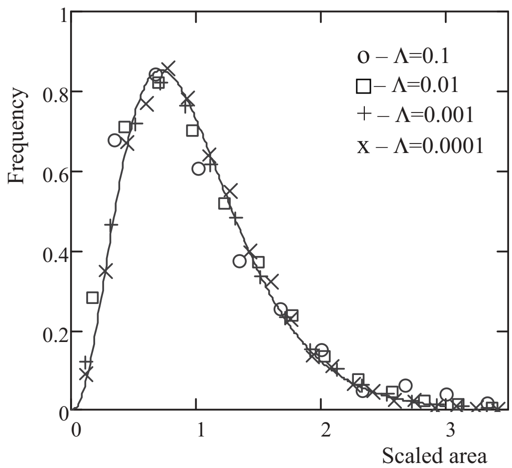

FIG. 1. Area distributions of the random domains (symbols) in comparison with the Kiang conjecture (solid line, $c = 3.575$).

Figure 2 shows kinetic curves computed as the number of tiles with the multiplicity 1 that form the free boundary at each step s (normalized to the total number of nuclei). With the decrease of nuclei density, the maximum on kinetic curves is shifted right and upward. In Fig. 3, these curves are scaled to the curve analytically calculated for the corresponding continual analog [22]:

$$L(r) = 4\sqrt{2}r\exp(-2r^2\lambda), \tag{3}$$

where r is the radius of the growing square nucleus (proportional to time) and λ is the conventional nuclei density (density of points, not tiles). The fit is acceptable for all values of Λ; at $\Lambda = 0.1$, it is somewhat worse. At this density, the normalized free boundary length equals 3.35 (<4) even at the very first step, which means the impingement of about 16% of all nuclei. In other words, even the first step of growth is not completely unrestricted. The model under study includes three

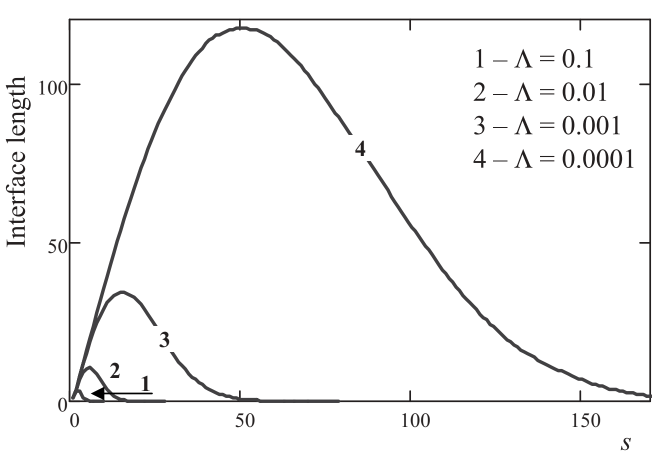

FIG. 2. Kinetic curves of tessellations with different densities of nuclei Λ.

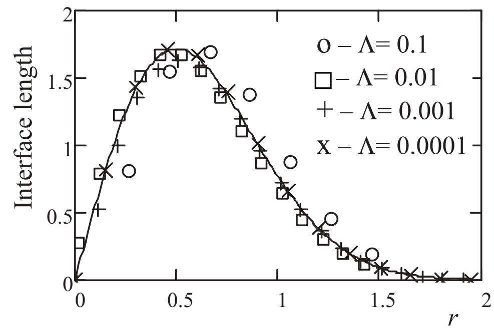

FIG. 3. The kinetic curve for the continual analog of considered tessellations (solid line, $\lambda = 1$) and scaled kinetic curves from Fig. 2 (symbols).

main processes: nucleation, unrestricted growth, and growth restricted by impingements. If there is no unrestricted growth because of the too-large density of nuclei, this is a different model. This determines a reasonable upper limit for Λ. The normalized free boundary length at the first growth step should be about 4.

In the case of hexagonal and triangular tilings, the situation is the same: in the whole range of studied values of Λ the area distributions are well approximated by the function Eq. (1) with $c = 3.575$, and the kinetic curves may be scaled one into another and into the kinetic curve of the corresponding continual analog provided that only tiles with the multiplicity 1 are taken into account.

In previous computations [20–22], neighbors were determined as follows. For each tile of the tiling, distances in the appropriate metric to all nucleation tiles were computed and the minimal distance was identified. Then the number of these minimal values in the array of distances was determined. This is the multiplicity of a tile (the number of equidistant nuclei). Two nucleation tiles were considered as neighbors if they had at least two common boundary tiles irrespective of their multiplicity. If they had only one common boundary tile (vertex), they were not neighbors. A detailed analysis of dense tessellations revealed that this criterion is ambiguous. In quite a number of cases, it selects nuclei that actually are not neighbors. Moreover, it is difficult, if possible, to suggest an unambiguous algorithm capable of determining actual neighbors in dense random tessellations after the growth process is completed.

To conclude, the presented results show that the scaling properties of the area distribution functions and kinetic curves hold for discrete tessellations on the whole studied range of Λ, and its apparent violation is rooted in the mentioned computational difficulties. To get more detailed characteristics of discrete random tessellations, neighbors need to be determined during the simulation of the growth process.

This research was partly supported by the Ukrainian Minister of Education and Science through Grant No. 0110U001453.

[1] P. A. Mulheran and D. A. Robbie, Europhys. Lett. **49**, 617 (2000).
[2] P. A. Mulheran, in *Handbook of Metal Physics 5*, edited by J. A. Blackman (Elsevier, Amsterdam, 2008).
[3] J. W. Evans and M. C. Bartelt, Phys. Rev. B **66**, 235410 (2002).
[4] M. Tomellini and M. Fanfoni, Phys. Rev. E **85**, 021606 (2012).
[5] M. Fanfoni, L. Persichetti, and M. Tomellini, J. Phys.: Condens. Matter **24**, 355002 (2012).
[6] E. A. Lazar, J. K. Mason, R. D. MacPherson, and D. J. Srolovitz, Phys. Rev. Lett. **109**, 095505 (2012).
[7] F. Ratto, T. W. Johnston, S. Heun, and F. Rosei, Surf. Sci. **602**, 249 (2008).
[8] L. Zaninetti, Phys. Lett. A **373**, 3223 (2009).
[9] M. Tanemura, Forma **18**, 221 (2003).
[10] H. J. Hilhorst, J. Stat. Mech. (2009) P05007.
[11] J.-S. Ferenc and Z. Neda, Physica A **385**, 518 (2007).
[12] P. Calka, Adv. Appl. Probab. **35**, 863 (2003).
[13] P. Calka and T. Schreiber, Ann. Probab. **33**, 1625 (2005).
[14] E. Pineda, V. Garrido, and D. Crespo, Phys. Rev. E **75**, 040107(R) (2007).
[15] E. Pineda and D. Crespo, J. Stat. Mech. (2007) P06007.
[16] E. Pineda and D. Crespo, Phys. Rev. E **78**, 021110 (2008).
[17] A. Gabrielli, J. Stat. Mech. (2009) N07001.
[18] A. V. Teran and A. Bill, Phys. Rev. B **81**, 075319 (2010).
[19] J. M. Rickman, Physica A **389**, 5155 (2010).
[20] A. Korobov, Phys. Rev. E **84**, 021602 (2011).
[21] A. Korobov, Phys. Rev. E **79**, 031607 (2009).
[22] A. Korobov, Phys. Rev. B **76**, 085430 (2007).
[23] T. Kiang, Z. Astrophys. **64**, 443 (1966).
[24] E. Pineda, P. Bruna, and D. Crespo, Phys. Rev. E **70**, 066119 (2004).
[25] J. D. Axe and Y. Yamada, Phys. Rev. B **34**, 1599 (1986).
[26] J. Farjas and P. Roura, Phys. Rev. B **75**, 184112 (2007).
[27] J. A. Blackman and P. A. Mulheran, Comput. Phys. Commun. **137**, 195 (2001).
[28] J. W. Evans, P. A. Thiel, and M. C. Bartelt, Surf. Sci. Rep. **61**, 1 (2006).
[29] M. Tomellini and M. Fanfoni, Int. J. Nanosci. **9**, 1 (2010).
[30] G. Eising and B. J. Kooi, Phys. Rev. B **85**, 214108 (2012).